Research on an Analytical Method for the Forming Force of External Spline Cold Roll-Beating

Qun Ma* – Xiangwei Zhang

Xi'an Technological University, School of Ordnance Science and Technology, China

To determine the force and energy parameters of cold roll-beating of external splines, the characteristics of the deformation zone in cold roll-beating are analysed. The geometric dimensions and position of the deformation zone change with the movement of the roller, the contact arc, and the reduction are very small, and there is an incomplete deformation zone in the initial stage of cold roll-beating. A discrete analytical method for calculating the unit pressure and deformation force is proposed, and the cold roll-beating process is discretized into an infinite number of cold-rolling processes with complex sections. The discrete analytical model of unit pressure and deformation force is established, and the unit pressure value and its distribution characteristics are determined. To verify the discrete analytical model, a finite element model of cold roll-beating is established, and the forming force is calculated. A horizontal milling machine is modified to carry out the cold roll-beating experiment, and the forming force is measured. The predicted results of the discrete analytical model are compared with the simulation and experiment results. The results show that the maximum error of radial force compared with the simulation and experiment results is about 7 % and 4 % respectively, and the variation curve of radial force is basically consistent, but the time of a cold roll-beating process is slightly shorter. The discrete analytical model correctly predicts the magnitude and change process of cold roll-beating forming force.
Keywords: discrete analytical method, cold roll-beating, forming force, deformation zone, radial force

Highlights
- *The changing characteristics of the metal deformation zone of external spline cold roll-beating are defined.*
- *A discrete analytical model for calculating the forming force of cold roll-beating is established by using the principal stress method.*
- *The finite element simulation of the cold roll-beating is carried out, the deformation of the workpiece is presented, and the forming force of the cold roll-beating is calculated.*
- *The cold roll-beating forming force is measured via experiment, and the discrete analytical model is verified. The results show that the discrete analytical model correctly predicts the magnitude and the change process of cold roll-beating forming force.*

0 INTRODUCTION

The cold roll-beating of external splines is a non-cutting manufacturing technology in which a pair of rollers with the same profile and the tooth space shape of the workpiece continuously strike the workpiece to produce plastic deformation to form a defined tooth shape. This kind of processing technology aiming at net or near net forming has been rapidly developed and plays an important role in industry. The processing efficiency of cold-rolling splines is very high, and it is widely used in the automobile and agricultural machinery industries.

The cold roll-beating process of splines is a discontinuous and progressive local deformation process, so the deformation mechanism is complex, and the theoretical analysis and parameter calculation are difficult. The research on this kind of problem is mainly carried out by experiments or finite element simulations.

Wu et al. [1] and Liu et al. [2] analysed the gear cold-rolling process with the finite element method and carried out experimental verification. Ma et al. [3]

analysed the gear roll-forming process with the finite element method and calculated the forming force. Fu et al. [4] used DEFORM-3D software to study the local induction heating rolling method, which is used to manufacture large gears. Zhang et al. [5] Quan et al. [6] and Wang et al. [7] used ABAQUS and ANSYS to conduct numerical simulations of the spline cold roll-beating process and calculate the deformation force of cold rolling. Wang et al. [8] established the finite element model for deformation prediction of the split straight bevel gear, and the results of finite element calculation were in good agreement with the experimental results. Yuan et al. [9] used ABAQUS to conduct finite element simulations of racks' cold roll-beating deformation force and then analysed the influence of materials, cold roll-beating speed, and cold roll-beating mode on the deformation force through experiments. However, the finite element analyses (FEA) of the complex profile rolling required a long central processing unit (CPU) time and large storage space. For example, a typical CPU time for the 3D FEA of gear rolling with a flat die was about one week, using DEFORM code in 2007 [10].

*Corr. Author's Address: Xi'an Technological University, No. 2 Xuefu Middle Road, Xi'an, China, 250239614@qq.com

409

The analytical model (e.g., modelled by the principal stress method or slip-line field method (SLFM)) has a clear physical interpretation and with shorter computation time. Zhang et al. [11] developed and improved the slip line field (SLF) and the analytical models of rolling force. Li et al. [12] and Li et al. [13] established the slip line field of external spline rolling forming and calculated the unit pressure and rolling pressure. Zhang et al. [14] developed an SLFM model with different friction models to analyse the spline cold-rolling process. Quagliato and Berti [15] established a slip line model for force estimation in the radial-axial ring rolling process. Then, the SLFM model was perfected to include axial force, by which experimental and numerical verifications were carried out [16]. Ma et al. [17] proposed an analytical model for predicting the pitch error of gear rolling with consideration of geometric relations and process parameters.

Although the above research has greatly improved the efficiency, the analytical model for the special forming process of external spline cold roll-beating has not been studied. At present, there is no analytical model, empirical formula, or chart for calculating the unit pressure and deformation force of external spline cold roll-beating.

In this paper, the characteristics of the cold roll-beating deformation zone are analysed, and the discrete analytical method for calculating the forming force is given. A cold roll-beating process is discretized into an infinite number of cold-rolling processes, and the unit pressure and deformation force of each cold-rolling process are calculated to determine the deformation force variation curve of a cold roll-beating process. Finally, the correctness of the discrete analytical method is verified via finite element simulation and cold roll-beating experiment.

1 FORMING PRINCIPLE OF EXTERNAL SPLINE COLD ROLL-BEATING

The tooth shape of an external spline is distinct, as is the cold roll-beating process. The involute spline is generally formed by continuous indexing, while the rectangular spline and triangle spline are formed by intermittent indexing.

Fig. 1 shows the principle of involute spline cold roll-beating. The cold roll-beating of an involute spline is carried out by continuous indexing at normal temperature. Two rollers rotate synchronously and reversely at high speed, and the angular velocity is ω_g. The rollers beat the workpiece once every revolution. The workpiece rotates continuously with the angular

velocity ω_p and feeds along the axis with the velocity v. During the contact time with the workpiece, two rollers rotate along their own rotation axis under the action of friction, and the angular velocity is ω_r. The transmission system of the machine tool strictly ensures that the ratio of ω_g to ω_p is the number of spline teeth so as to process the involute keyway, which is consistent with the profile of the roller section.
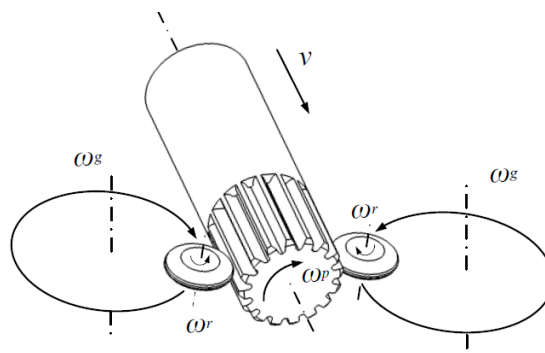
Fig. 1. *Schematic diagram of cold roll-beating of involute spline*

2 CHARACTERISTICS OF THE METAL DEFORMATION ZONE OF COLD ROLL-BEATING

In this paper, a cold roll-beating process is defined as the process of the roller from contacting the workpiece to leaving the workpiece in a rotation cycle. In a cold roll-beating process, the rotation speed and feed speed of the workpiece are far less than the rotation speed of the rollers, and the contact time between the rollers and the workpiece is very short (several milliseconds); it can be approximately considered that the workpiece is stationary when the rollers beat it.

The cold roll-beating is similar to a metal rolling process, and the research on metal rolling theory is more developed, which can provide theoretical guidance for the calculation of the forming force of cold roll-beating. However, the cold roll-beating is different from the general metal rolling process, as the location and parameters of the metal deformation zone are changing constantly.

Fig. 2 shows the variation of the metal deformation zone. O is the rotation centre of the roller. R is the radius of rotation of the roller axis. r is the radius of the roller. h_f is the rolling depth. Arc DE and $D'E'$ are the profile curves of the section formed by two cold roll-beating processes on the same tooth space. P is the axial feed rate of the workpiece per revolution.

It can be seen from Fig. 2a that the position of the deformation zone is not fixed but moves continuously with the roller. When the roller is at B_1, the contact arc, bite angle and reduction are arc A_1B_1, α_1 and Δh_1. When the roller moves to B_i, the contact arc, bite angle and reduction change to arc A_iB_i, α_i and Δh_i. When the roller moves to the other position on the arc $D'E'$, all of the above deformation zone parameters are different. Considering the profile shape of the roller, the average width of the deformation zone at different positions on the arc $D'E'$ is also different. According to the geometric relationship in Fig. 2a, when the spline modulus is small, the contact arc length and the reduction are also small relative to the workpiece thickness.

It can be seen from Fig. 2b that D' is not the starting point of the cold-rolling process. When the roller is at B on the extension line of arc $D'E'$, the cold-rolling process begins, but the deformation zone is not complete at this time. The theoretical contact arc, bite angle and reduction are arc AB, α and Δh. Due to the missing part, the actual deformation zone parameters are arc AB', α' and $\Delta h'$. However, the duration of the incomplete deformation zone is very short. The length of the contact arc, the bite angle and the reduction increase rapidly and reach the maximum when the roller moves to D', then decrease slowly and decrease to 0 at E'.

Therefore, there are three main characteristics of a cold roll-beating metal deformation zone. First, the location and parameters of the deformation zone are constantly changing; Second, there is an incomplete deformation zone in the initial stage of cold rolling; Third, the contact arc and the reduction are both small.

In the process of metal deformation, it is impossible to calculate the forming force directly by the principal stress method with the change in the geometric size of the deformation zone.

3 ESTABLISHMENT OF THE DISCRETE ANALYTICAL MODEL

A cold roll-beating process is different from a metal rolling process, but it is similar when the rollers only rotate along their own rotation axis ($\omega_g = 0$). The periodic rotation of the roller only changes the position and geometric parameters of the deformation zone.

As shown in Fig. 2a, when the roller is located at B_1, assuming that $\omega_g = 0$ and $\omega_r > 0$, the cold roll-beating process can be approximately regarded as the cold-rolling process of the workpiece along the direction of $C'C$ in the following time, in which the workpiece is rolled in at A_1 and rolled out at B_1, and the rolling speed is expressed as

$$V_1 = r\omega_{r1}, \tag{1}$$

When the roller moves to point B_i, the cold roll-beating process can also be approximately regarded as a cold-rolling process from A_i to B_i, and the rolling speed is expressed as

$$V_i = r\omega_{ri}, \tag{2}$$

Because the rotation angular velocity of the roller is constant at any time, $V_1 = V_i$.
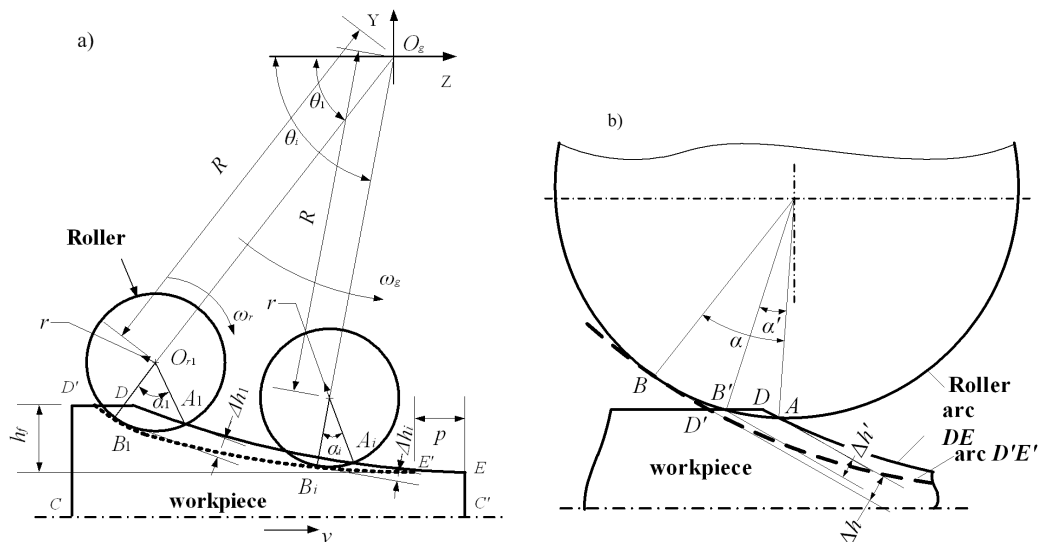
Fig. 2. *The change of metal deformation zone in cold rolling; a) complete deformation zone; and b) incomplete deformation zone*

Since there is no other external force in the cold-rolling process, a cold roll-beating process can be discretized into an infinite number of tension-free cold-rolling processes of a complex cross-section with the same rolling speed.

Fig. 3 shows the force condition of any differential unit in the metal deformation zone. Firstly, it is very important to determine the direction of friction t_z, which determines the type of deformation zone. The 3D solid model of the workpiece and the roller was established by using the Solidworks 3D design software, and it was imported into the pre-processing program of the finite element software DEFORM-3D. The rotation speed of the roller is set to 209 rad/s, and the radius of rotation is 90 mm. To simulate the forming force in a cold roll-beating process, the contour formed by the last cold roll-beating is directly established on the workpiece, as shown in Fig. 4.
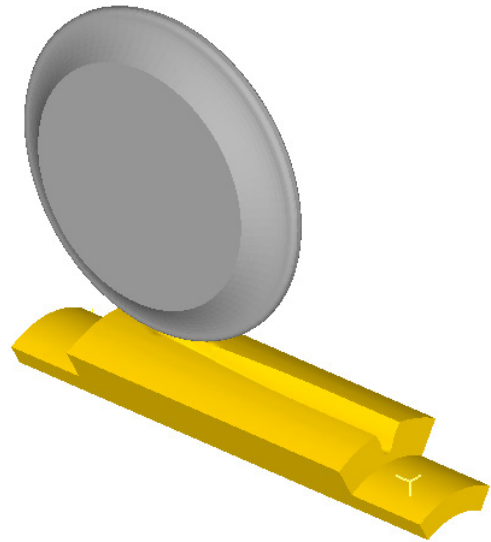
Fig. 4. *The finite element model of cold rolling*

Observe the velocity nephogram of metal particles, as shown in Fig. 5. The finite element analysis shows that at any time of cold roll-beating, the metal flow velocity in the deformation area is less than the linear velocity of the roller, so the whole deformation area belongs to the backward slip zone, and the direction of friction on the contact arc is opposite to the linear velocity of the roller.

As shown in Fig. 3, if the elastic deformation of the roller and the workpiece is neglected, the sum of the components of the force acting on the differential unit along the Z direction is expressed as

$$p_z \sin \varphi_z \frac{dz}{\cos \varphi_z} + \sigma_z y - t_z \cos \frac{dz}{\cos \varphi_z}$$

$$-(\sigma_z - d\sigma_z)(y + dy), \qquad (3)$$

Fig. 3. *Force condition of any differential unit in deformation zone of workpiece*
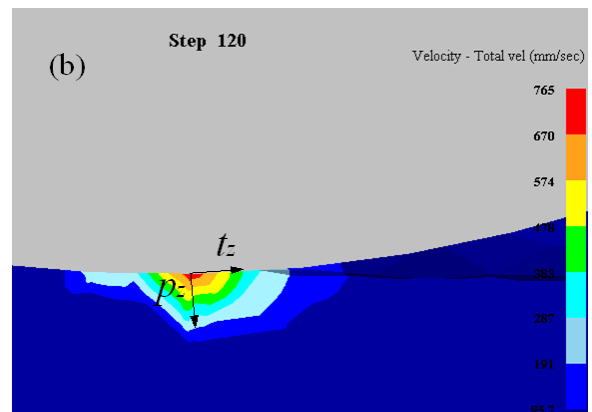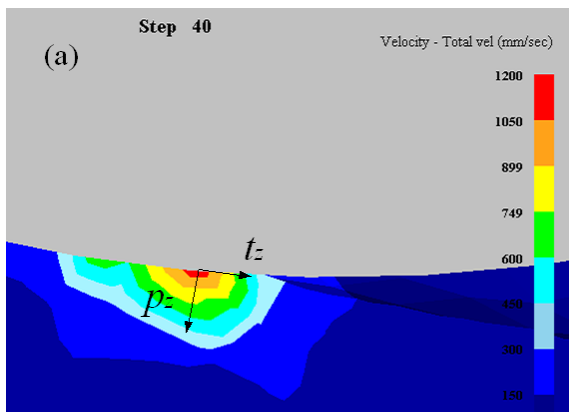
Fig. 5. *Velocity nephogram of metal particles at a) step 40, and b) steep 120; in [mm/s]*

where p_z is the unit pressure of the roller on the workpiece, and T_z is the unit friction force between the roller and workpiece. If z and y are the coordinates of the contact arc, then $\tan(\varphi_z) = dy/dz$, which can be substituted into Eq. (3), and the Kalman differential equation for calculating the average unit pressure is obtained, expressed as

$$\frac{dp_z}{dz} - \frac{K}{y}\frac{dy}{dz} - \frac{t_z}{y} = 0, \tag{4}$$

where K is determined by the plastic equation under plane deformation, expressed as

$$K = \sigma_1 - \sigma_3 = \frac{2}{\sqrt{3}}\sigma, \tag{5}$$

where σ_φ is the actual deformation resistance of the metal.

Assuming that the contact friction condition in the deformation zone obeys the dry friction law, i.e., $t_z = fp_z$, where f is the friction coefficient on the contact arc, the solution of the differential Eq. (4) is as follows

$$p_z = e^{\int \frac{f}{y}dz}\left(C + \int \frac{K}{y}e^{\int \frac{f}{y}dz}dy\right), \tag{6}$$

where C is integral constant determined by boundary conditions.

Since the difference between the contact arc and the chord connecting the roll-in point and the roll-out point is very small, the contact arc can be approximated to a chord as

$$dz = \frac{l_a}{\Delta h}dy, \tag{7}$$

where l_a is the length of chord AB.

Substitute Eq. (7) into Eq. (6) and integrate them, and determine the integral constant according to the tension-free boundary condition. Finally, the distribution formula of unit pressure is obtained as

$$p_z = \frac{K}{\delta}\left[(\delta-1)\left(\frac{h+\Delta h}{y}\right)^\delta + 1\right]. \tag{8}$$

Here, $\delta = \frac{l_a f}{\Delta h}$, and h is half of the thickness of the workpiece at the rolling point.

If the workpiece is an involute spline with $Z=20$ and $m=2$ mm, the cold roll-beating parameters are $p=1$ mm, $r=20$ mm, $R=90$ mm, and the friction coefficient on the contact arc is $f=0.17$. After the deformation zone parameters such as h and l_a are determined from Fig. 2, the unit pressure on the contact arc and its distribution along the Y direction can be determined by Eq. (8).

Fig. 6 shows the distribution of unit pressure along Y direction on the contact arc in a single cold-rolling process. It can be seen that the distribution of unit pressure is not uniform. As the roller moves towards point E' (Δh becomes smaller), the unit pressure on the contact arc decreases, which is due to the decrease of the reduction and the length of the contact arc. The unit pressure on the contact arc is small in the whole cold roll-beating process because the length and reduction of the contact arc are very small.
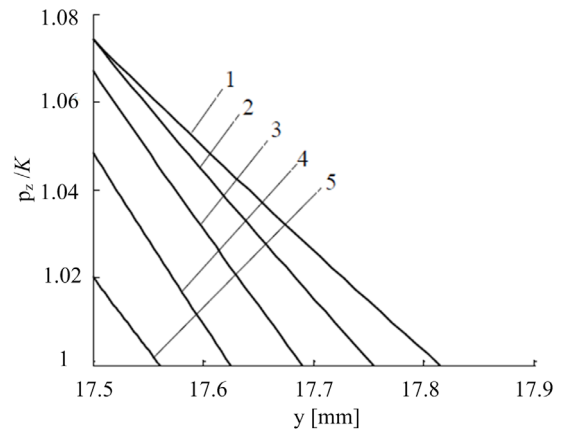
Fig. 6. *Distribution of unit pressure on contact arc:*
1 Δh = 0.31 mm; 2 Δh = 0.25 mm; 3 Δh = 0.19 mm;
4 Δh = 0.12 mm; 5 Δh = 0.06 mm

The unit pressure in the incomplete deformation zone should be calculated according to the parameters of the theoretical deformation zone. Although incomplete, the force condition of any differential unit in the deformation area is still as shown in Fig. 3.

According to the unit pressure obtained with Eq. (8), the deformation force of each cold-rolling process is calculated, so as to determine the deformation force and its changes during one cold roll-beating process.

The deformation force in each cold-rolling process can be decomposed into radial force and tangential force (i.e., the component of the deformation force along Y and Z directions).

It can be seen from Fig. 3 that the radial force can be determined by the following equation as

$$F_y = \bar{b}\cos\alpha \cdot n_\sigma \int_{Z_B}^{Z_A} p_z \frac{dz}{\cos\varphi_z}\cos\varphi_z$$

$$+ \bar{b}\sin\alpha \cdot n_\sigma \int_{Z_B}^{Z_A} t_z \frac{dz}{\cos\varphi_z}\sin\varphi_z, \tag{9}$$

where, $\bar{b}$ is the average width of the deformation zone, n_σ is the stress state coefficient, Z_A and Z_B are the Z-axis coordinates of points A and $\mathbf{B}$ in Fig. 3.

Since $\tan(\varphi_z) = dy/dz$ and $t_z = fp_z$, then

$$F_y = \bar{b}n_\sigma \int_{Z_B}^{Z_A} (p_z \cos\alpha \cdot dz + fp_z \sin\alpha \cdot dy). \quad (10)$$

Substitute Eqs. (5), (7) and (8) into Eq. (10), and the radial force can be expressed as

$$F_y = \bar{b}n_\sigma \cdot \frac{2\sigma_\varphi}{\sqrt{3}\delta} \left\{ \int_h^{h+\Delta h} \left(\frac{l_a}{\Delta h} \cdot \cos\alpha + f\sin\alpha \right) \cdot \left[(\delta - 1)\left(\frac{h+\Delta h}{y} \right)^\delta + 1 \right] dy \right\}. \quad (11)$$

After the integration, we can obtain the following equation as

$$F_y = \bar{b}n_\sigma \cdot \frac{2\sigma_\varphi}{\sqrt{3}\delta} \left(\frac{l_a}{\Delta h} \cdot \cos\alpha + f\sin\alpha \right) \cdot \left[h\left(\frac{h+\Delta h}{y} \right)^\delta - h \right]. \quad (12)$$

The analytical formula of tangential force can also be deduced as

$$F_z = \bar{b}n_\sigma \cdot \frac{2\sigma_\varphi}{\sqrt{3}\delta} \left(\cos\alpha - \frac{l_a}{\Delta h} \cdot f\sin\alpha \right) \cdot \left[h\left(\frac{h+\Delta h}{y} \right)^\delta - h \right]. \quad (13)$$

Therefore, the parameters of $\bar{b}$, n_σ and σ_φ must be determined when calculating the deformation forces.

4 DETERMINATION OF THE PARAMETERS

4.1 Determination of Average Width of the Deformation Zone

Considering the symmetry of the profile of the roller, the total pressure on the roller should point to the axis of the roller. Therefore, in the calculation, the width of the deformation zone $\bar{b}$ is taken as the width of the projection area along the total pressure direction of the actual deformation zone, so it is determined by the geometric relationship shown in Fig. 2a and the profile curve of the roller.

4.2 Determination of Stress State Coefficient n_σ

The stress state coefficient is affected by the size of the roller, external friction, external zone metal and tension, and can be expressed as

$$n_\sigma = n_\beta n'_\sigma n''_\sigma n'''_\sigma, \quad (14)$$

where n_β is the stress state coefficient considering the influence of workpiece width, n'_σ is the influence coefficient of external friction, n''_σ is the external zone influence coefficient, n'''_σ is the tension influence coefficient.

A cold roll-beating process is regarded as an infinite number of cold-rolling processes, while for small module spline, if the friction coefficient on contact arc is constant, the influence of n_β, n'_σ and n'''_σ can be ignored.

Since the length of contact arc and the reduction are very small, which is similar to thick workpiece rolling, considering the influence of the external zone on the average unit pressure, the external zone influence coefficient can be expressed as

$$n''_\sigma = \left(\frac{l_a}{h} \right)^{0.4}. \quad (15)$$

4.3 Determination of Actual Deformation Resistance of Metal

The actual deformation resistance is affected by the nature of metal, temperature, deformation degree and deformation speed. Several scholars [18] to [21] have studied the mathematical models of deformation resistance of various alloys in accordance with the characteristics of Chinese materials, which can be used to calculate the deformation force of cold roll-beating.

Studies show that the effect of strain rate on deformation resistance is relatively small at low temperature [18] and [19], so the effect of deformation rate is not considered in the calculation.

5 VERIFICATION OF THE DISCRETE ANALYTICAL MODEL

The accuracy of the discrete analytical method is verified by the finite element method and the experimental results. Because the effect of workpiece indexing is very small, the cold roll-beating forming force of rack is measured in the experiment.

5.1 Design of the Roller

It is more complicated to make the roller strictly according to the involute tooth profile, and the tooth shape does not affect the verification. To reduce the experimental cost, the roller with the tooth profile size as shown in Fig. 7 is made, and the maximum outer circle radius is $R = 24$ mm. To conform to the cold roll-beating process of rack, the roller is designed with three tooth profiles. After cold roll-beating, two complete teeth and three tooth spaces are formed on the workpiece.
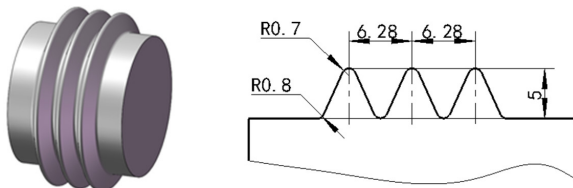
Fig. 7. *a) 3D model of the roller, and b) its profile size*

5.2 Establishment of Finite Element Model

In this paper, the discrete analytical model is used to calculate the forming force of a single tooth roller. Although the roller shown in Fig. 7 has three teeth, the parameters of the three deformation regions are the same, so the results of the discrete analytical model can be expanded three times to compare with the experimental results.

Consistent with the discrete analytical model, the roller is also modelled according to the shape of a single tooth, but the tooth shape is modified to the size shown in Fig. 7, and the tooth groove size on the workpiece is also modified accordingly. Import the 3D models into DEFORM-3D preprocessor, and the symmetry plane of the tooth groove is $X = 0$, as shown in Fig. 8.
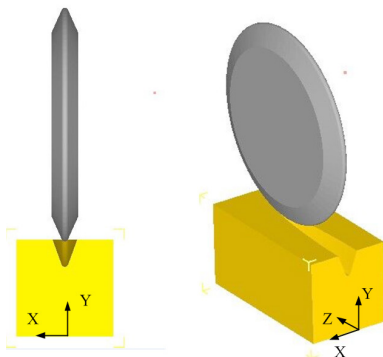
Fig. 8. *The finite element models of the roller and workpiece*

5.3 Reformation of Experimental Equipment

In this paper, a horizontal milling machine is reformed, and the roller is installed on the spindle, as shown in Fig. 9. The spindle motor power is 7.5 kW, the spindle speed is 30 r/min to 1500 r/min, and the feed motor power is 1.5 kW. The radial and tangential forces of cold roll-beating are measured with a PCB261A03 tri-axial forces sensor, which is produced by PCB Piezotronics INC in the United States.
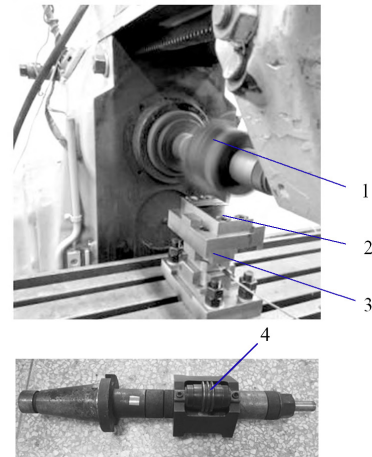
Fig. 9. *Cold roll-beating experimental equipment;*
1 machine tool spindle, 2 workpiece,
3 triaxial forces sensor, and 4 the roller

5.4 Selection of Workpiece Material

The difference of materials only affects the actual deformation resistance of metals but does not affect the verification of the discrete analytical model. Because the horizontal milling machine is not specifically defined as cold roll-beating equipment, the stability and the power are insufficient, so the workpiece material is selected as copper with good ductility and small deformation resistance.

6 RESULTS AND DISCUSSION

6.1 Measurement of Cold Roll-Beating Forming Force

If the cold roll-beating process with the feed of 2 mm/r is tested, the nearest speed should be selected according to the speed ratio of the horizontal milling machine gearbox, and it should also meet the load requirements of the motor. The experimental parameters are as follows: the cold roll-beating depth is 2.5 mm, the roller rotation speed is 25.13 rad/s (240 r/min), and the workpiece feed speed is

476 mm/min (feed rate 1.983 mm/r). Samples formed by cold roll-beating are shown in Fig. 10.

Change curves of radial and tangential forces measured in the experiment are shown in Fig. 11. As shown in Fig. 11a, the radial force increases continuously in the beat-in stage and remains constant in the stable stage (about 31.8 kN) and decreases continuously in the beat-out stage. As shown in Fig. 11b, the maximum tangential force is only about 2 kN, which is about 6.3 % of the maximum radial force.
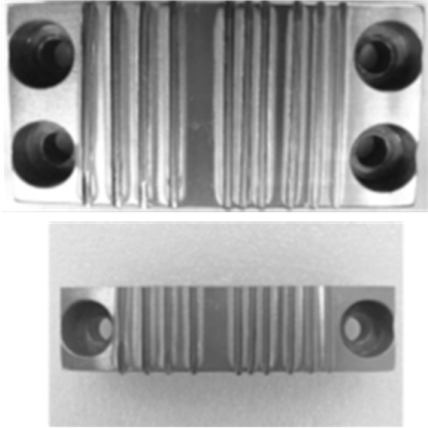
Fig. 10. *Samples formed by cold roll-beating*
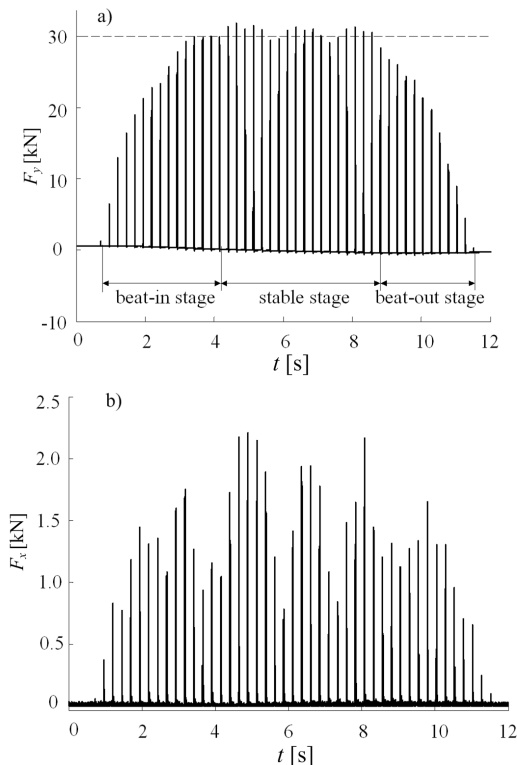
Fig. 11. *Cold roll-beating forming forces measured in the experiment; a) the radial force; b) the tangential force*

6.2 Finite Element Simulation of Cold Roll-Beating

6.2.1 Preprocessing of Finite Element Models

The parameters in the DEFORM-3D preprocessor are set as follows:

1. Without considering the influence of deformation of the roller, the roller is considered as a rigid body, the workpiece is considered as a plastic body. The material of workpiece is set to BRASS-CDA-110 in the DEFORM-3D material library, and is considered with a constant property in room temperature (20 °C);
2. A ring region with thickness of 5 mm of workpiece is refined with density ratio of 2, as shown in Fig. 12;
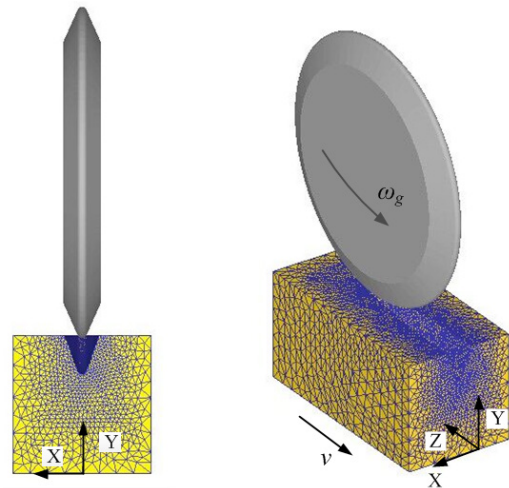
Fig. 12. *Preprocessing of finite element models*

3. The element number is 39192, and minimum element size is about 0.6574 mm;
4. Without considering the rotation of the roller, the roller rotates around the spindle with an angular velocity of 25.13 rad/s, and the feed speed of the workpiece is 476 mm/min (feed rate 1.983 mm/r);
5. In the process of cold roll-beating, it can be considered as pure rolling between the roller and the workpiece. To simplify the calculation, the friction coefficient between the roller and the workpiece is set to 0;
6. The target volume option is set to active in FEM + meshing.

6.2.2 Finite Element Simulation Results

In the DEFORM-3D postprocessor, the distribution of the effective stress and the contact state are

given, as shown in Fig. 13, where the green nodes represent the contact nodes. The distribution area of the effective stress and contact nodes moves with the roller, indicating that the position of the deformation zone is also moving constantly. The distribution area of contact nodes and the variation of stress are increasing and then decreasing, which indicates that the parameters of metal deformation zone are also changing. The results in Fig. 13 validate the analysis of the characteristics of the deformation zone of cold roll-beating in this paper.

Fig. 14a shows the deformation of the tooth groove. Compared with previous deformation, the width of the tooth groove significantly increases, and the increments along the workpiece feed direction (Z direction) also show a trend of increasing and then decreasing, which indicates the trend of variation in the width of the deformation zone. Fig. 14b shows the variation curves of forming force; it can be seen that the maximum radial force is about 10.9 kN, while the maximum tangential force is about 0.8 kN, which is about 7.3 % of the maximum radial force,

which is basically consistent with the experimental measurement results. The reason that the tangential force is very small is that the deformation on both sides of the tooth groove is distributed symmetrically along the centre of the tooth groove, as shown in Fig. 14a. Therefore, the tangential force on both sides of the tooth groove is equal in magnitude and opposite in direction.

6.3 Comparison of Cold Roll-Beating Forming Force

Since the radial force of cold roll-beating is much larger than the tangential force, only the radial force is considered when calculating the forming force with the discrete analytical model. At the stable stage in Fig. 11, the radial force variation curve of a cold roll-beating process is obtained and compared with the discrete analytical model calculation results and the finite element simulation results, as shown in Fig. 15. In the experiment, the roller contains three teeth, so the calculation results and simulation results are expanded by three times for comparison.
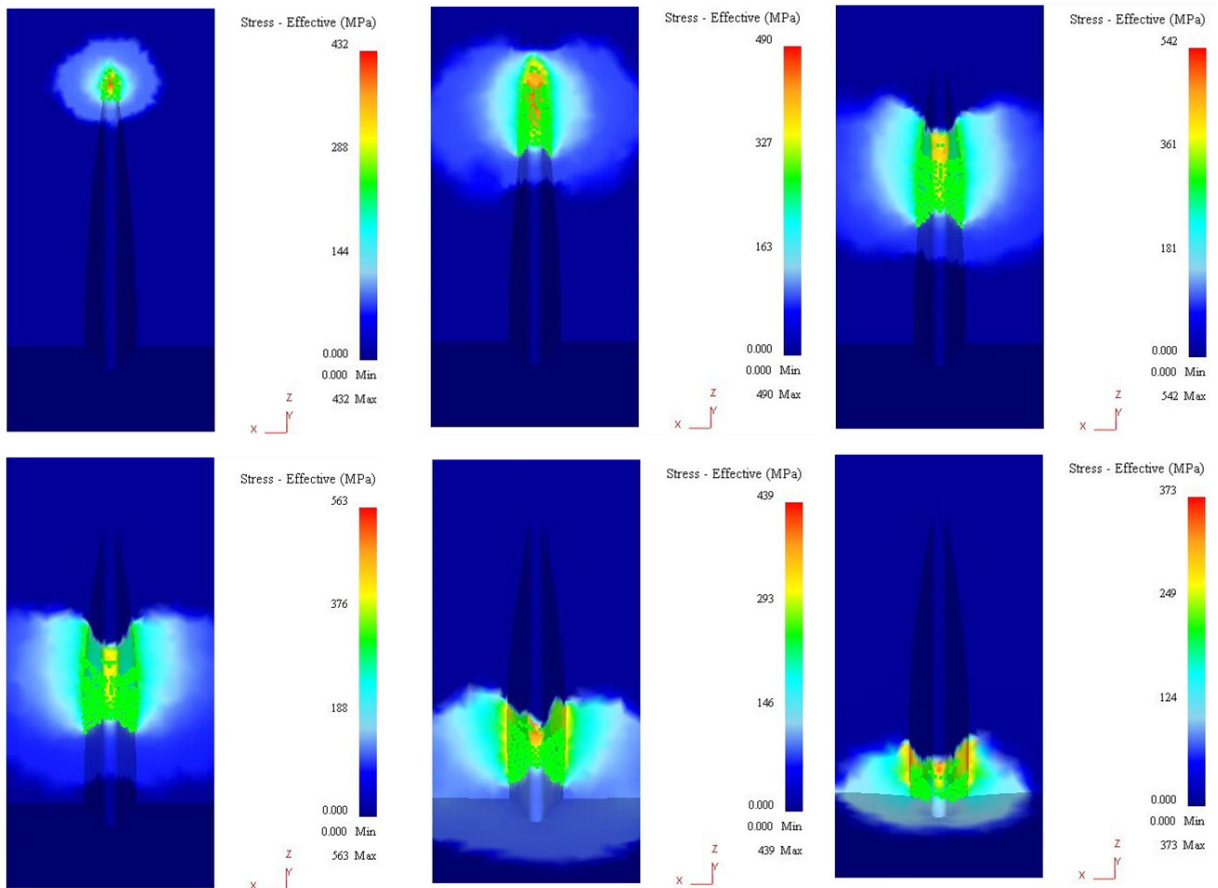
Fig. 13. *Effective stress distribution and contact state on the workpiece*
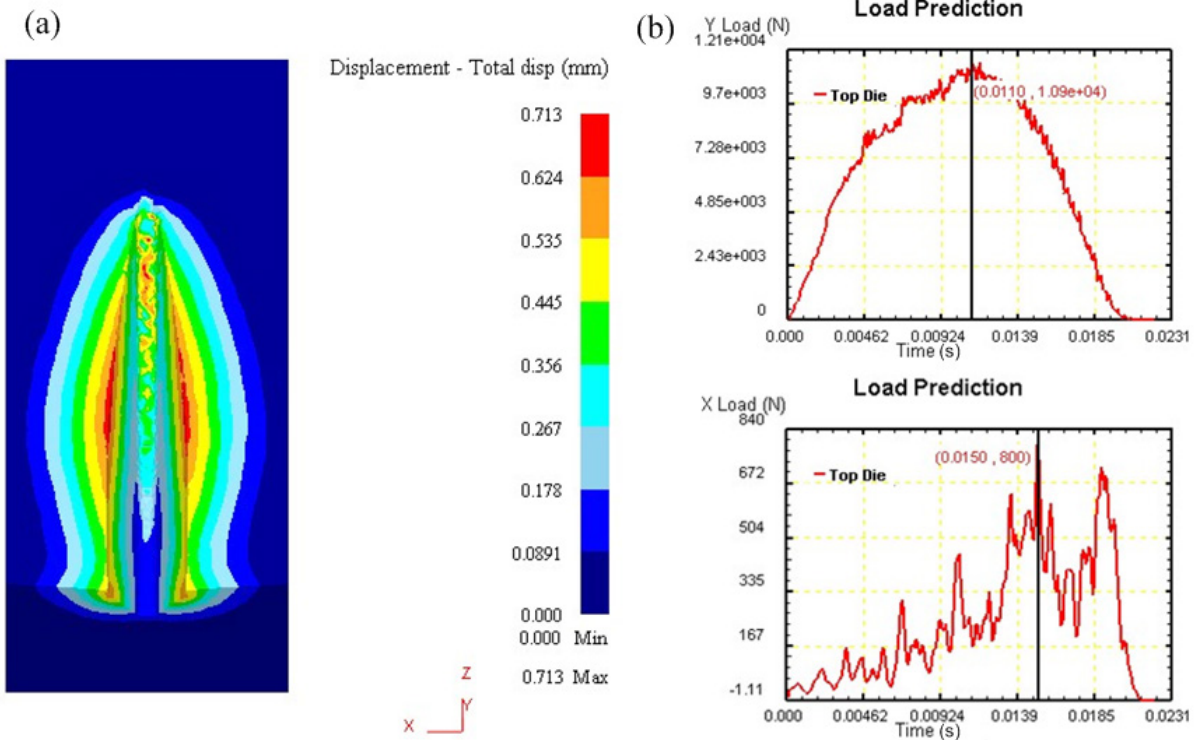
Fig. 14. *Deformation of the tooth groove and the forming force*

It can be seen from Fig. 15 that the maximum value of radial force predicted by the discrete analytical model is 30.5 kN, which is about 2.2 kN different from the simulation results (about 32.7 kN) with an error of 7 %, and only about 1.3 kN different from the experimental measurement results at the stable stage (about 31.8 kN) with an error of 4 %.

The change trend of radial force predicted by the discrete analytical model is approximately the same as that of simulation and experimental results, but there is an error when the maximum radial force is reached.

The duration of cold roll-beating process predicted by the discrete analytical model is in good agreement with the simulation results but significantly less than the experimental results.
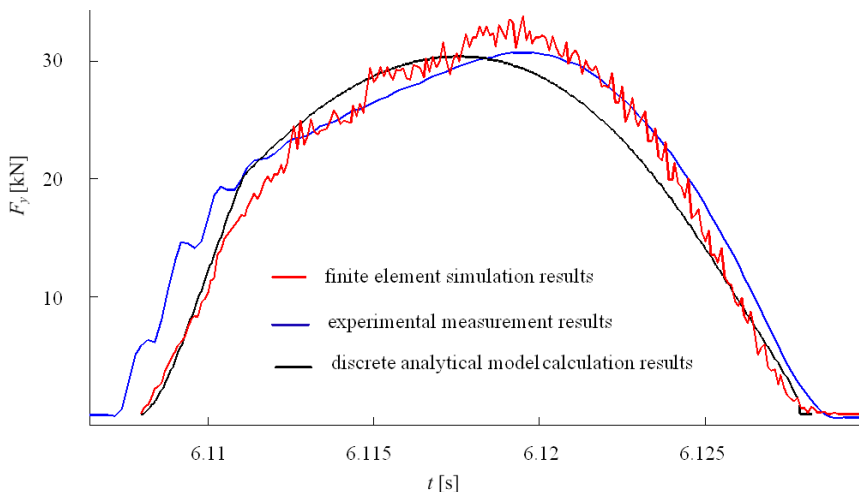
Fig. 15. *Comparison of cold roll-beating radial force calculated by different methods*

6.4 Reasons for the Longer Duration of Cold Roll-Beating Measured in Experiment

The action process of the roller on the workpiece is similar to the plastic problem of the wedge or cylinder sliding over the smooth surface. Research on this kind of problem has shown that the slip line field in the metal deformation zone should be as shown in Fig. 16 (V_r is the instantaneous linear velocity of the roller) [22] to [24]. As the cold roll-beating progresses, the friction coefficient increases [25], and the metal bulge in front of the roller, so the time of cold roll-beating is longer.

Similar results can be seen in the finite element simulation. The workpiece is cut by $X = 0$ plane, and the deformation of the metal at the bottom of the groove is obtained, as shown in Fig. 17. The metal bulge in front of the roller is obvious, and a protrusion is formed on the beat-out face, and a collapse is formed on the surface. Since the tooth groove formed by the last cold roll-beating has been established on the 3D model of the workpiece, the protrusion and the collapse are not obvious after simulation, and the duration of cold roll-beating process is not increased.

However, in the experiment, the tooth groove is formed after multiple cold roll-beating, so the protrusion is more obvious, and the duration is longer.

At the same time, the elastic recovery of metal, the insufficient stiffness and the lack of power of machine tools will also increase the time of cold roll-beating.

Although there is some error in the time of cold roll-beating process calculated by the discrete analytical method, it does not affect the determination of cold roll-beating force and energy parameters. Cutting fluid is used in cold roll-beating, and the adhesion of metal can be controlled, and the stability and power of the special cold roll-beating machine tools are more appropriate, so the theoretical value will be closer to the true value.

6.5 Prospects for Future Research

Although the discrete analytical model can predict the cold roll-beating forming force quickly and accurately, it cannot do so with some factors, such as the elastic deformation of the roller, the bulge and collapse of the metal material. The finite element simulation
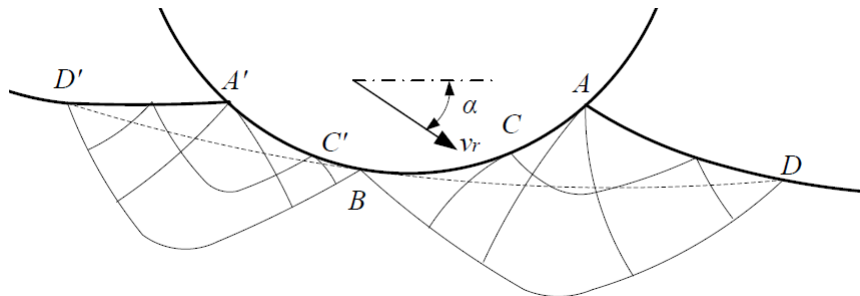
Fig. 16. *Slip line field in the metal deformation zone of cold roll-beating*
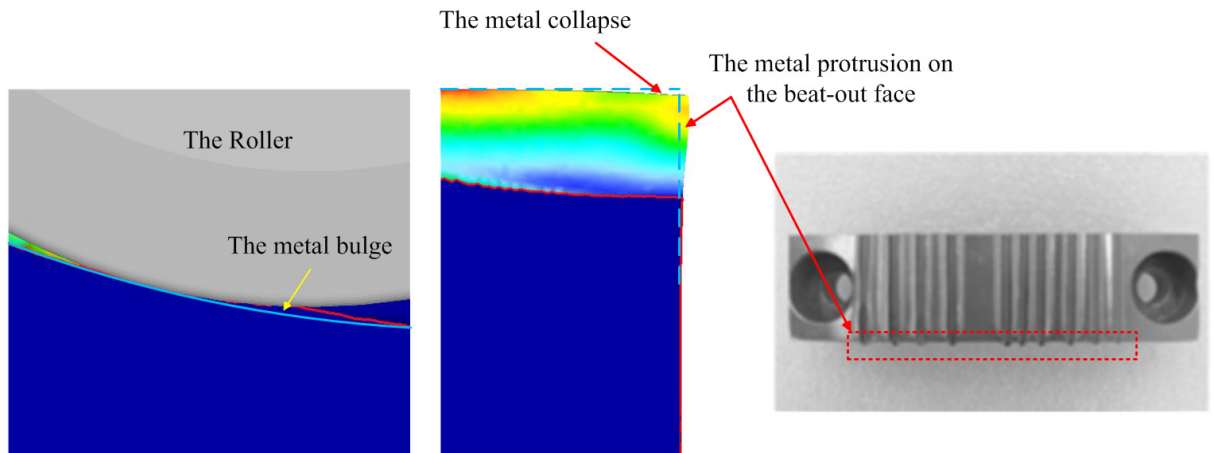
Fig. 17. *The bulge, collapse, and protrusion of metal*

consumes significant simulation time, but it provides the movement process of the metal deformation zone more intuitively, and shows the shape of the metal during and after deformation more completely.

In the future, the research work on the forming force of cold roll-beating should be combined with the finite element simulation method to simulate the whole cold roll-beating process to form a complete tooth groove, study the influence of the metal shape after deformation on the forming force, study the influence of elastic deformation of roller, and further improve the discrete analytical model.

7 CONCLUSIONS

1. The characteristics of deformation zone in cold roll-beating are analysed. The position and parameters of the deformation zone are constantly changing. The contact arc length and reduction are very small, and there is an incomplete deformation zone in the initial stage of cold roll-beating.

2. The discrete analytical model of unit pressure and deformation force in cold roll-beating is established. A cold roll-beating process is discretized into an infinite number of cold-rolling processes. The unit pressure of each cold-rolling process is calculated. The deformation force of cold roll-beating is calculated.

3. The change curves of cold roll-beating forming force are obtained by finite element simulation and experimental measurement. The results show that the change trend of cold roll-beating forming force predicted by the discrete analytical model is basically consistent with that of finite element simulation and experimental measurement. The maximum calculation error compared with the simulation and experiment results is about 7 % and 4 % respectively. The discrete analytical method is accurate in predicting the cold roll-beating forming force.

8 REFERENCES

[1] Wu, T., Wang, G., Li, J., Yan, K. (2018). Investigation on gear rolling process using conical gear rollers and design method of the conical gear roller. *Journal of Materials Processing Technology*, vol. 259, p. 141-149, **DOI:10.1016/j.jmatprotec.2018.04.034**.

[2] Liu, Z., Song, J., Li, Y., Li, X. (2011). Analysis and experimental study on cold-rolling precision forming process of involute spline. *Journal of Mechanical Engineering*, vol. 47, no. 14, p. 32-38. **DOI:10.3901/JME.2011.14.032** (in Chinese).

[3] Ma, Z., Luo, Y., Wang, Y., Mao, J. (2018). Geometric design of the rolling tool for gear roll-forming process with axial-infeed. *Journal of Materials Processing Technology*, vol. 258, p. 67-79, **DOI:10.1016/j.jmatprotec.2018.03.006**.

[4] Fu, X., Wang, B., Zhu, X., Tang, X., Ji, H. (2016). Numerical and experimental investigations on large-diameter gear rolling with local induction heating process. *The International Journal of Advanced Manufacturing Technology*, vol. 91, p. 1-11, **DOI:10.1007/s00170-016-9713-y**.

[5] Zhang, L., Li, Y., Yang, M., Yuan, Q. (2012). Finite element numerical simulation of high speed cold roll forming process. *Materials for Mechanical Engineering*, vol. 36, no. 8, p. 86-88, **DOI:10.1007/s11783-011-0280-z** (in Chinese).

[6] Quan, J., Cui, F., Yang, J. (2008). Numerical simulation of involute spline shaft's cold-rolling forming based on ANSYS / LS-DYNA. *China Mechanical Engineering*, vol. 19, no. 4, p. 419-422 (in Chinese).

[7] Wang, X., Xu, H., Cui, F. (2007). Finite element simulation of spline cold rolling forming. *Mining Machinery*, vol. 35, no. 9, p. 139-141 (in Chinese).

[8] Wang, B., Yan, C., Li, J., Feng, P., Wang, S., Chen, S., & Su, J. (2021). Residual Stress and Deformation Analysis in Machining Split Straight Bevel Gears. *Strojniški vestnik - Journal of Mechanical Engineering*, vol. 67, no. 3, p. 114-122, **DOI: 10.5545/sv-jme.2020.7064**.

[9] Yuan, Q., Li, Y., Yang, M. (2014). Research on deformation force of block material in cold roll forming. *China Mechanical Engineering*, vol. 25, no. 2, p. 251-256, **DOI:10.3969/j.issn.1004-132X.2014.02.022** (in Chinese).

[10] Kamouneh, A.A., Ni, J., Stephenson, D., Vriesen, R., DeGrace, G. (2007). Diagnosis of involutometric issues in flat rolling of external helical gears through the use of finite-element models. *International Journal of Machine Tools and Manufacture*, vol. 47, no. 7-8, p. 1257-1262, **DOI:10.1016/j.ijmachtools.2006.08.015**.

[11] Zhang, D., Zhao, S., Ou, H. (2016). Analysis of motion between rolling die and workpiece in thread rolling process with round dies. *Mechanism and Machine Theory*, vol. 105, p. 471-494, **DOI:10.1016/j.mechmachtheory.2016.07.008**.

[12] Li, Y., Zhang, D., Fu, J. (2007). Unit average pressure in cold rolling forming process of external spline. *China Mechanical Engineering*, vol. 18, no. 24, p. 2977-2980, **DOI:10.3321/j.issn:1004-132x.2007.24.018** (in Chinese).

[13] Li, R., Song, J., Li, Y. (2007). Calculation of rolling force in cold rolling forming of external spline. *Shanxi Metallurgy*, vol. 30, no. 6, p. 10-15, **DOI:10.3969/j.issn.1672-1152.2007.06.004** (in Chinese).

[14] Zhang, D., Xu, F., Yu, Z., Lu, K., Zheng, Z., Zhao, S. (2021). Coulomb, Tresca and Coulomb-Tresca friction models used in analytical analysis for rolling process of external spline. *Journal of Materials Processing Technology*, vol. 292, **DOI:10.1016/j.jmatprotec.2021.117059**.

[15] Quagliato, L., Berti, G.A. (2017). Temperature estimation and slip-line force analytical models for the estimation of the radial forming force in the RARR process of flat rings. *International Journal of Mechanical Sciences*, vol. 123, p. 311-323, **DOI:10.1016/j.ijmecsci.2017.02.008**.

[16] Quagliato, L., Berti, G.A., Kim, D., Kim, N. (2018). Slip line model for forces estimation in the radial-axial ring rolling process. *International Journal of Mechanical Sciences*, vol. 138-139, p. 17-33, **DOI:10.1016/j.ijmecsci.2018.01.025**.

[17] Ma, Z., Luo, Y., Wang, Y. (2018). On the pitch error in the initial stage of gear roll-forming with axial-infeed. *Journal of Materials Processing Technology*, vol. 252, p. 659-672, **DOI:10.1016/j.jmatprotec.2017.10.023**.

[18] Zhou, J., Wang, Z., Gao, Y., Lun Y. (1994). Flow stress mathematical model of aluminum alloy. *Journal of Beijing University of Science and Technology*, vol. 16, no. 4, p. 351-356 (in Chinese).

[19] Guan, K., Fan, B., Zhou, J. (1996). Experimental study on thermal deformation of brass. *Acta Metallurgica Sinica*, vol. 32, no.7, p. 749-754, **DOI:CNKI:SUN:JSXB.0.1996-07-011** (in Chinese).

[20] Dai, Z., Zhou, J., Zhang, S. (1997). A mathematical model for flow stress of copper alloy in cold state. *Nonferrous Metals*, vol. 49, no. 2, p. 88-91, **DOI:CNKI:SUN:YOUS.0.1997-02-018** (in Chinese).

[21] Zhang, S., Dai, Z., Zhou, J. (1997). Mathematical model of cold flow stress for aluminum alloy. *Journal of Beijing University of Science and Technology*, vol. 19, no. A02, p. 65-68, **DOI:CNKI:SUN:BJKD.0.1997-S1-01** (in Chinese).

[22] Challen, J.M., Oxley, P.L.B. (1984). Slip-line fields for explaining the mechanics of polishing and related processes. *International Journal of Mechanical Sciences*, vol. 26, no. 6, p. 403-418, **DOI:10.1016/0020-7403(84)90030-4**.

[23] Busquet, M., Torrance, A.A. (1999). Investigation of surface deformation and damage when a hard cylindrical asperity slides over a soft smooth surface. *Tribology Series*, vol. 36, p. 101-109, **DOI:10.1016/S0167-8922(99)80032-7**.

[24] Hill, R. (1950). *The Mathematical Theory of Plasticity*. Oxford University Press, Inc., New York.

[25] Zhang, H., Wang, M. (1989). Effect of aluminum adhesion on rolling friction coefficient. *Light Alloy Processing Technology*, vol. 9, p. 17-19 (in Chinese).